CHAPTER 1: INTRODUCTION

1.1 Overview of Childhood Cancer

Cancer is a general term for the abnormal growth of cells. Cancer begins when normal cells start to transform and undergo abnormal cell division. Cancer occurrence in children is relatively rare. Childhood cancers have different histological types compared to adults.

Table 1.1: Cancer incidence rates in children by different age group in the United States

Cancer Type	Age Group and Incidence Rate per 100,000				
	<1	1-4	5-9	10-14	15-19
All cancer types	23.6	20.3	11.2	12.7	21.6
Leukemia	4.3	8.3	3.5	2.8	2.7
Brain and other central nervous system	3.4	3.9	3.2	2.5	2.1

The rates of age are adjusted to the 2000 U.S. standard population. The statistics are obtained from Centers for Disease Control and Prevention and National Cancer Institute. (Group, 2005)

Between the years 2003-2005, the Malaysian Cancer Registry reported a cancer incidence of 67,792 per 100,000 populations in Peninsular Malaysia; of which 0.05% were children aged between the ages 0-19 years. In the United States, approximately 10,400 children under the age of 15 years were diagnosed with cancer and about 1,545 children were predicted to die from the disease in the year 2007 (Garcia, 2007).

Among the 12 major types of childhood cancers, leukemia (cancer of blood cells), and cancers of the brain and central nervous system account for more than half of new cases per year. Approximately one-third of childhood cancers are leukemia and the most common type of leukemia is acute lymphoblastic leukemia. The most common solid tumours are brain tumours (e.g., gliomas and medulloblastomas), with other tumours such as neuroblastomas and Wilms tumours, and sarcomas (rhabdomyosarcoma and osteosarcoma) being less common. (Carroll & Finlay, 2010).

The etiology of childhood cancers is still not clear. Although leukemia is ultimately a disease of the DNA, no single mutation has been linked to childhood ALL. The cytogenetic abnormalities frequently found in ALL cases include germ-line karyotypic abnormalities, somatic karyotypic abnormalities, translocations, and deletions. Germ-line abnormalities like Down syndrome (trisomy 21), Bloom syndrome, Fanconi anemia, Klinefelter syndrome, and ataxia -telangiectasia have been associated with an increased risk of developing childhood leukemia. Somatic abnormalities associated with childhood leukemia include aneuploidy (in one form or another in 92% of childhood ALL cases),

pseudodiploidy (in 41.5% of ALL cases) and hyperdiploidy (in 20–30% of pre-B ALL and about 90% of early precursor-B cell ALL) (Wartenberg, Groves, & Adelman, 2008).

Another cytogenetic abnormality observed in childhood ALL is the presence of oncogene fusion transcripts that arise from chromosomal translocation. Translocations in ALL cases include the t (12; 21)/*TEL-AML1* translocation (most common in childhood leukemia) and t (4; 11)/*MLL-AF4* gene fusion (very common in infant ALL). Other prognostically important translocations include t (1; 19) which gives rise to *E2A-PBX1* fusion translocation and t (9; 22), the Philadelphia chromosome which leads to the *BCR-ABL* fusion transcript.

Environmental factors have been suspected by many scientists to be a cause of childhood cancer but this has been difficult to prove, partly because cancer in children is rare and because it is difficult to identify past exposure levels in children. Radiation (ionizing and nonionizing), solvents, pesticides, outdoor air pollution, tobacco smoke, diet and maternal pharmaceutical use have been proposed as exposure candidates due to consistent epidemiological evidence (Estey, Faderl, Kantarjian, MyiLibrary, & SpringerLink, 2008).

The most widely accepted theory of causation of childhood ALL is based on an infectious etiology associated with decreased immune function. The three variations of this theme on "infection" that have been put forward are:

(1) exposure to a specific infectious agent postnatally (Kinlen, 1988) ,

(2) exposure to a specific infectious agent prenatally (Smith et al., 1998), or

(3) a delay in the initial exposure to infectious agents in general beyond the first year of life, (Greaves & Alexander, 1993) .

Despite the belief that viral infections play a pivotal role in the development of childhood leukemia, no specific virus has been conclusively linked to its etiology and neither is there evidence of viral genomic inclusions within leukaemia cells. (McNally & Eden, 2004)

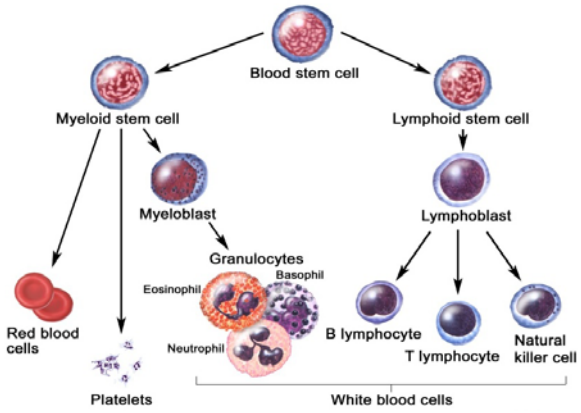

Figure 1.1: White blood cells. Figure shows formation of white blood cells, red blood cells and platelets from blood stem cell (Winslow, 2007).

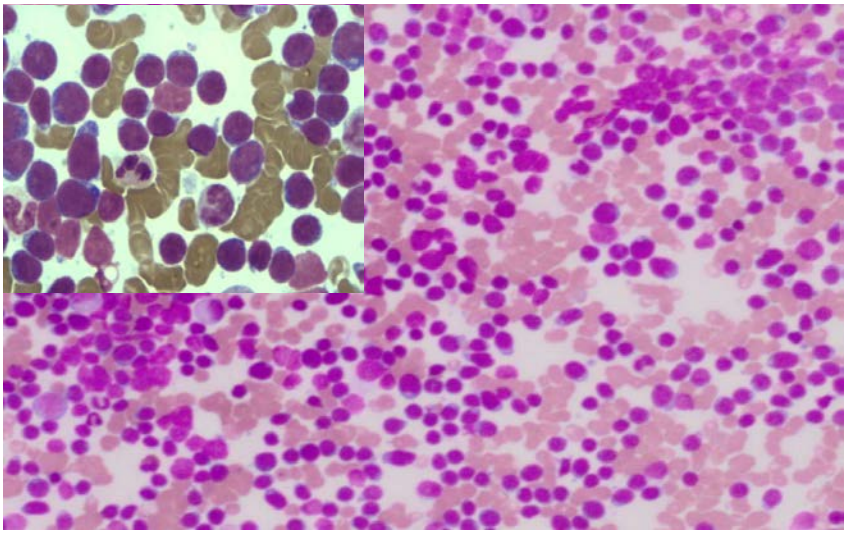

Figure 1.2: Lymphoblasts. Figure shows bone marrow diffusely replaced by lymphoblasts (100X, MGG stain), (inset). Heterogeneous lymphoblasts of FAB-L2 morphology with high nuclear:cytoplasmic ratio with some displaying characteristic "mirror-handle" shape (400X).

1.2 Telomere

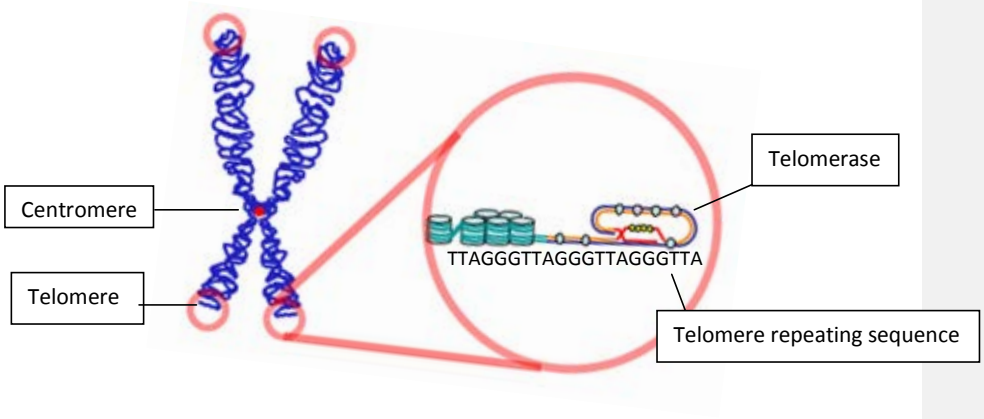

Figure 1.3: Human Telomeres. Figure shows human chromosomes with a zoom in structure of telomere structure. (Peggy, 2009)

Telomeres are specialized structures at both ends of all eukaryotic cell chromosomes. Telomeres have G-rich repeats in 5'-3' strands of each eukaryote. Every vertebrate has telomere that is composed of thousands of repetitive TTAGGG DNA sequences while other species have different G-rich sequences, e.g., Tetrahymena has TTGGGG (S.E. Artandi & R.A. DePinho, 2010). In humans, the length of telomere repeats

is about 15-20kb at birth and about 8-10kb in adults. The exact length of the telomere varies by individuals, organs, cells and even among chromosomes.

Telomeres play an important role in protecting the chromosome ends from DNA degradation, DNA repair mechanisms, and fusion. The ends of the chromosomes have to be capped because a “bare” state can activate the DNA damage response and cause end-to-end fusion that results in cellular senescence, apoptosis, and further chromosomal instability (Artandi & DePinho, 2010)

1.3 Telomerase

Telomerase, also known as telomere terminal transferase is an enzyme that elongates chromosomes by adding TTAGGG sequences to the end of existing chromosomes. Human telomerase is composed of a catalytic component of telomerase reverse-transcriptase (*TERT*) (Cerni, 2000) and a telomerase RNA component or human telomerase RNA (*TERC*), used to extent telomeres. Telomerase can elongate the G-rich 3’ telomere overhang using *TERC* as the template. (Blackburn, 2001; Lange, 2005).

In cancer cells, telomerase activity is usually associated with the proliferation state of the cells. This enzyme is vital for infinity proliferation (immortality) and its absence leads to finite lifespan (senescence) of the cell.

1.4 Telomere Repeat Binding Factor 2 (TERF2)

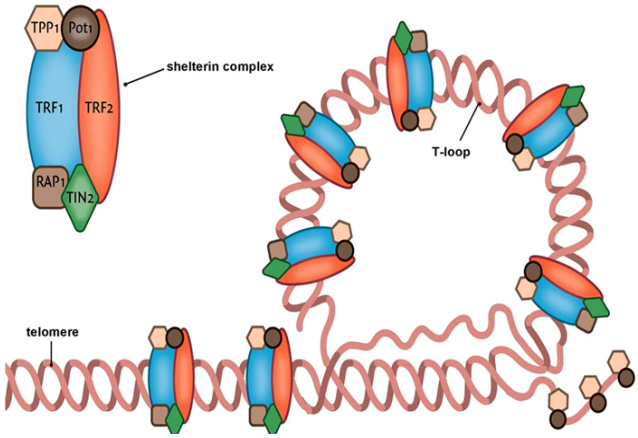

Figure 1.4: Telomere structure with T-loop formation. The shelterin complex consists of the following proteins: 'telomere repeat binding factor' (*TERF2*) 1 and 2, '*TERF2*1 interacting nuclear protein 2' (*TIN 2*), 'repressor activator protein 1' (*RAP 1*) and the 'protection of telomere 1' (*POT 1*). (Huzen, de Boer, van Veldhuisen, van Gilst, & van der Harst, 2010).

Telomere Repeat Binding Factor 2 (*TERF2*) can directly bind to TTAGGG repeats and interacts with other factors to form a large protein complex. *TERF2* is one of the components of the sheltering complex (telosome) composed of *TERF1*, *TERF2*, *TINF2*,

TERF2IP ACD and *POT1*. The *TERF2* gene encodes a telomere specific protein TERF2, which is an important telomere nucleoprotein complex. *TERF2* plays a key role in the protective activity of telomeres.

TERF2 will bind to the telomeric double-stranded TTAGGG repeats. The binding protects the telomere from end-to-end fusion of chromosomes. Furthermore, it plays a role in successful progression through the cell division cycle. A component of the shelterin complex the, telosome is also involved in the regulation of telomere length and protection. Without shelterin, telomeres are no longer hidden from the DNA damage surveillance and wrong chromosome ends are chosen for DNA repair pathways.

1.5 Significance of Telomere in cancer

Telomeres have been found to be abnormal in many cancer cell lines (Lange et al., 1990; Hastie et al., 1990). In addition, telomerase activities have been reported to be increased in 80-90% of cancers (Kim et al., 1994; Stewart & Weinberg, 2006). An alternative telomere lengthening will take place when the telomerase activity is very low. It is known as Alternative Lengthening of Telomeres (ALT) mechanism (Dunham, Neumann, Fasching, & Reddel, 2000). The mechanism will be activated to produce infinite replicating capacity of cancer cells.

Short telomeres have also been reported to be associated with cancer. Continuous telomere shortening in the absence of telomerase could eventually result in a short telomere length.

Short telomeres lead to high chromosomal instability which is also a characteristic of human tumours (Blasco, 2005).

Chapter 2 – LITERATURE REVIEW

2.1 Childhood ALL

2.1.1 Background

Leukemia is the commonest cancer in children (47.6 %) (Jemal, Siegel, Xu, & Ward, 2010). The term leukemia was first introduced by Virchow in 1847, which prior to this, was only recognized as unusual white blood cell disease (Pui, 2006). In the past 30 years, progress in leukemia studies has grown parallel with the development of many new technologies.

Leukemia is a malignant disease of blood-forming cells in the bone marrow. These deranged, immature cells accumulate in the blood and within organs of the body. They are not able to carry out the normal functions of blood cells. There are two major types of leukemia, myelogenous and lymphocytic, both having acute and chronic forms.

Acute lymphoblastic leukemia (ALL) is the most common pediatric cancer. Seventy five percent of all newly diagnosed leukemia and 25% of all cancers in children are ALL (Kaatsch, 2010). ALL occurs when many under-developed white blood cells known as lymphoblasts are found in the peripheral blood and bone marrow (Rees, 1997). ALL can develop in two forms; de novo ALL, which is when the malignancy is diagnosed for the first time, or relapse ALL which is the return of malignancy after an remission from treatment. The treatment of acute lymphoblastic leukemia has undergone tremendous

improvement in the medical world and ranked as one of the most successful advances in the battle against cancer.

Figure 2.1: Ten most frequent cancers in males by the age 0-14 in Peninsular Malaysia. (Lim & Halimah, 2006)

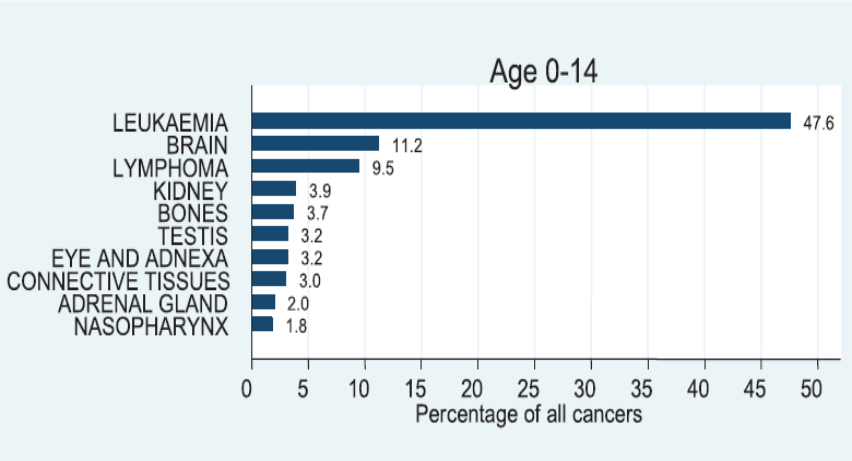

Figure 2.2: Lymphoblastic leukemia according to age group and gender in Peninsular Malaysia between the years 2003 to 2005. (Lim & Halimah, 2006)

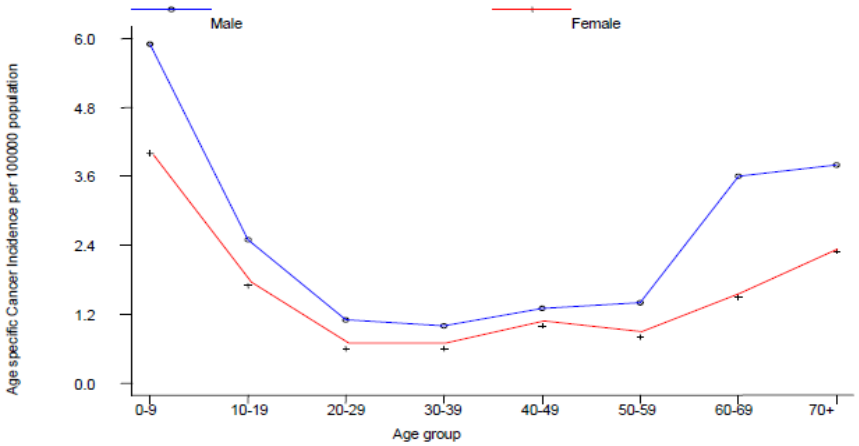

2.1.2 Clinical Presentation

The symptoms and signs of ALL vary between individuals. The duration of symptoms in children with ALL can range between days to months. There are cases where ALL progresses rapidly while in other types of leukemia, the initial signs and symptoms appear in a more sub acute manner that persists for months before diagnosis.

Children with ALL normally present with signs and symptoms of marrow failure (C.H. Pui, 2006) or the impact of bone marrow infiltration with leukemic cells which goes to the extent of extramedullary disease spread (Pizzo & Poplack, 2006). The first symptoms are usually non-specific and include anorexia, irritability and lethargy (Conter et al., 2004; Pizzo & Poplack, 2006). In addition, common constitutional symptoms include fever (60%), fatigue (50%), pallor (25%), and weight loss (25%) (Esparza & Sakamoto, 2005). Patients may also experience bone pain, which will normally affect the long bone which demonstrates leukemic involvement of the periosteum and bone. Young children may

present with limp or refusal to walk, bone tenderness and arthalgia which results from leukemic infiltration (Pizzo & Poplack, 2006).

Headache, vomiting, respiratory distress, oliguria and anuria can be classified as rare signs and symptoms. Enlargement of the liver or spleen, are normally observed (60-70%) at initial diagnosis. (Doctors Conter, Rizzari, Sala, Chiesa, & Citterio, 2004)

2.1.3 Pathobiology and pathophysiology

The hematologic origin in ALL development always undergoes the same event. It is believed to involve a transformation process that occurs in a single mutant hematopoietic progenitor cell that is capable for infinity clonal expansion (Esparza & Sakamoto, 2005; Pui, 2006). It results in malignant, poorly differentiated hematopoietic precursors. Leukemic transformation of hematopoietic cells requires subversion of the controls of normal proliferation, a block in differentiation, resistance to apoptotic signals, and enhanced self-renewal (C. H. Pui, Relling, & Downing, 2004).

The occurrence of leukemia may occur in mature lymphoid cells of B- or T-cell lineages or in early precursor cells (G. H. Reaman, 2002). This phenomenon results in the different subtypes of ALL, based on the stage of lymphoid differentiation of the cells.

The development of technology gives rise to a lot of new inventions in molecular study. Molecular characterization of genetic alterations in blast cells has contributed greatly to our understanding of the pathogenesis of this disease (Gilliland & Tallman, 2002). Genetic changes are responsible considerably to the genesis of the malignancy and of course give vital impact for its diagnosis and treatment (Ferrando & Look, 2000). Molecular

identification of genetic targets of the mutation has resulted in the discovery of numerous cancer and tumour suppressor genes, which can give important clues to the mechanism of leukemogenesis (Rowley, 2000).

The common oncogenic mechanisms include the abnormal expression of oncoproteins such as MYC, TAL1, LYL1, LMO2 and HOX11, and translocations between chromosomes that result in fusion of genes encoding active kinases (e.g. *BCR-ABL*) or altered transcription factors (e.g. *TEL-AML1*, *E2A-PBX1*, and *MLL* which linked to one of many fusion partners) (Liang & Pui, 2005).

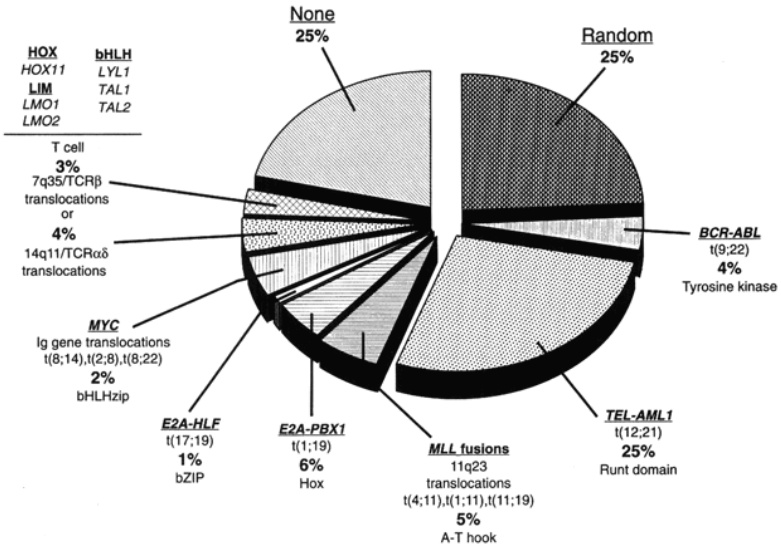

Figure 2.3: Distribution of translocation-associated oncogenes in childhood ALL. The majority of genes affected by chromosomal rearrangements encode proteins active in transcriptional regulation of cell growth, differentiation, or survival (Pui, 2006)

2.1.4 Prognosis

Certain criteria such as clinical and laboratory features have been used can be used as prognostic factors. The determination of these factors is very important in the modern therapeutic field. Age, sex, and initial leukocyte count are consistently cited as common prognostic factors for ALL (Esparza & Sakamoto, 2005). The initial WBC and age are two main prognostic factors. Initial WBC count is accepted as a prognostic indicator at diagnosis (Doctors Conter, et al., 2004). A linear relationship arises between initial leukocytes count and clinical outcome of ALL in children.

Children who have higher leukocytes counts tend to have a poor prognosis (Simone, Verzosa, & Rudy, 1975). T-cell ALL commonly presents with a high leukocyte count and has a high rate of lymphoblast proliferation (Bradbury, 2003; Plasschaert, Kamps, Vellenga, de Vries, & de Bont, 2004). In addition, age also plays an important role in the outcome of ALL in children. Regardless of the adjustment of other factors, age remains a highly vital predictor outcome. Children who are young at diagnosis (< 2 years) and older

patients (> 10 years) have a relatively poorer prognosis when compared to patients in the intermediate age range (W Crist et al., 1986; Sather, 1986).

2.2 Molecular Characterization

2.2.1 Numeric chromosomal changes

ALL can be classified into five subtypes based on the molecular number of the chromosomes; hyperdiploid with more than 50 chromosomes (25-30% of cases, including near-tetraploid, near triploid, and hyperdiploid with 51 to 68 chromosomes); hyperdiploid with 47 to 50 chromosomes (10-15% of cases); pseudodiploid (46 chromosomes with structural or numeric abnormalities; about 40% of cases); diploid (46 chromosomes; 10-15% of cases); and hypodiploid (fewer than 46 chromosomes; about 8% of cases, including near-haploid cases) (C.H. Pui & Crist, 1994). Ploidy has been shown to be a distinct cytogenetic feature in ALL that can be used to predict prognosis and stratify therapy.

2.2.2 Structural Chromosome changes

The most common rearrangements in the leukemic cells of pediatric patients with ALL are the translocations namely t(12;21), t(1;19), t(4;11), and t(8;14) (Chessells, 2000). Other chromosomal regions, such as 6q, 7q35, 8q24.1, 9p, 12p13, 14q11.2, 11q23, and 21q22,

undergo translocations, deletions, and inversion with numerous partners. Although uncommon recurrent chromosomal rearrangements associated with ALL have been identified in small subgroups of patients, this research focuses on the more common structural abnormalities and their likely contribution to the disease process.

TEL-AML1

TEL-AML1 fusion is the most frequent cytogenetic lesion for children with B-lineage ALL which is about 25%. The *TEL-AML1* fusion is created by the t (12; 21). The fusion is not observed by conventional cytogenetic banding methods but it is easily detected by FISH or RT-PCT methods (Harrison et al., 2005).

TEL is located at 12p13 and is a member of the ETS (Expressed Tagged Sequence)-like family of transcription factors. It plays an important role as a regulator of hematopoietic-cell development, which is vital for normal haemopoeisis (Hock et al., 2004). *AML1* is located on the chromosome region 21q22. The gene is essential for normal hematopoietic development (Okuda, van Deursen, Hiebert, Grosveld, & Downing, 1996).

TEL-AML1 expression is linked with a good clinical outcome, with event-free survival rates approaching 90% (Borkhardt et al., 1997). Thus, patients with *TEL-AML1* are expected to have a superior prognosis compared to the other subtypes.

BCR-ABL

BCR-ABL is the first oncogene fusion described in ALL. It results from the reciprocal translocation between chromosomes 22 and 9, i.e.: t(9;22)(q34;q11). The fusion oncogene is also known as the 'Philadelphia (Ph) chromosome'. Cytogenetic studies have reported the incidence of the Ph chromosome in about 3% to 5% of pediatric ALL cases (Crist et al., 1990). However, in Asian patients as high as 7% *BCR-ABL* positive in ALL cases have been reported (Ariffin et al., 2007).

BCR breakpoints on chromosome 22 are grouped in two areas: a 5.8-kb major breakpoint cluster region (M-bcr) in CML and a minor breakpoint cluster region (m-bcr) in most cases of childhood Ph-positive ALL (Groffen et al., 1984). Fusion genes created by breaks in M-bcr (CML-type break) encode a 210-kilodalton (kDa) fusion protein (p210), whereas fusions that occur in m-bcr (ALL-type break) encode a 190-kDa protein (p190) (Kaeda, Chase, & Goldman, 2000).

In childhood ALL, the *BCR-ABL* fusion gene is associated with an older age group, a higher leukocyte count, and more frequent central nervous system (CNS) leukemia at diagnosis (Rubnitz & Crist, 1997) Cases with *BCR-ABL* expression have an extremely poorly prognosis despite treatment with contemporary therapy (Pui 2006).

The outcome for adult and pediatric patients with Ph+ ALL is poor on current treatment protocols (Cazzaniga et al., 2002) with 4-years event-free survival (EFS) rates of approximately 30% despite intensive chemotherapy (Uckun et al., 1999).

E2A-PBX1

The fusion gene for *E2A-PBX1* is t(1;19)(q23;p13). It is present in about 6% of all B-lineage ALL and in 25% of cases with a pre-B (cytoplasmic immunoglobulin-positive) immunophenotype (Pui, 2006). *E2A* generates the best-characterized chimeric transcription factor in ALL whose activities illustrate the importance of homeo-domain, or HOX, proteins in leukemogenesis.

E2A-PBX1 has multiple ways for the growth of cancer cell. *E2A-PBX1* is connected with HOX family members and modifies the transactivation activity of these complexes. A vital component of *E2A-PBX1*-mediated tumour development is associated with the activation of gene transcription. RT-PCR assay was developed due to molecular characterization of the translocation t(1;19) (Borowitz et al., 1993; Privitera et al., 1992).

Patients with *E2A-PBX1* fusions have poor outcome on antimetabolite-based therapies but response well to increased dosage of the treatment (Pui & Crist, 1992; Raimondi et al., 1990; Rivera et al., 1991).

MLL –AF4

The Mixed Lineage Leukemia (*MLL*) gene is located on the chromosome 11, band 11q23 (Libura, Ward, Solecka, & Richardson, 2008). The cytogenetic lesion is found in 2 to 3% of all pediatric ALL cases. The fusion is detected in 50% to 70% of infants. Most of the translocations at 11q23 alters the MLL gene (Ziemin-Van Der Poel et al., 1991).

Cell signaling genes have been localized to 11q23. The *MLL* gene is one of the genes on 11q23 which is most often rearranged. They are also called as *ALL1*, *HRX*, and *HTRX*.

Molecular techniques to detect *MLL* rearrangements include Southern blot analysis, fluorescence in situ hybridization (FISH), and RT-PCR. Although less sensitive than RT-PCR, Southern blots or FISH can detect essentially all *MLL* rearrangements, regardless of the partner gene involved (Rubnitz et al., 1994).

2.3 Telomerase Binding Factor TERF 2

2.3.1 Role and expression of *TERF2 in Cancer*

The shelterin complex consists of six members (Dimitrova, 2009). The main two factors are *TERF1* and *TERF2*. They play an important role in recruiting and stabilizing other shelterin members by binding to the double-stranded portion (M. Blasco, 2005). *TERF2* is also known as telomere-binding protein. It has a vital role in telomere protection and telomere-length regulation. A lot of research has been conducted on *TERF2*. It has been shown that *TERF2* is up-regulated in some human tumours and plays an important part in cancer (Blanco, Muñoz, Flores, Klatt, & Blasco, 2007).

The *TERF2* complex protects the telomeric single-stranded G-rich overhang from degradation and from DNA repair activities. The protection thereby restrains telomere end-to-end fusions (Ahmad & Henikoff, 2002). Mutations are observed in *TERF2*-interacting

telomeric proteins. They are characterized by premature aging, prone to cancer and shortening of telomerases to below the critical length (M. Blasco, 2005).

TERF2 is detectable in most tissues but is highly expressed in spleen, thymus, prostate, uterus, testis, small intestine, colon and peripheral blood leukocytes (Yanai et al., 2005) in humans. *TERF2* is over expressed in a variety of epithelial malignancies including lung, skin and breast cancer.

CHAPTER 3: PATIENTS AND METHODS

3.1 Project Outline

3.1.1 Patient and control samples

Expression of *TERF2* in different types of hematological malignancies was studied. The results were compared with control samples (without the disease). The control bone marrows were selected from healthy donors and also patients with non-malignant disease. The number of samples for each type of cancer is shown in the table below.

Table 3.1: Patients and control bone marrow samples at diagnosis.

Diagnosis	*Number of patients*
B – ALL *(fusion gene)*:-	
TEL-AML1	10
BCR-ABL	8

E2A-PBX1	3
MLL gene rearrangement	1
Negative OFT	50
Relapses	3
AML	7
CML	1
Solid Tumours	5
Control	9
Total	97

Table 3.2: Three bone marrow and six peripheral blood samples used as controls

No	***Sample type***	***Diagnosis***
1	Peripheral blood	Viral hepatitis
2	Peripheral blood	Healthy donor
3	Bone marrow	Healthy donor
4	Bone marrow	Healthy donor
5	Bone marrow	Langerhans cell histiocytosis
6	Peripheral blood	Viral infection
7	Peripheral blood	Healthy donor
8	Peripheral blood	Healthy donor
9	Peripheral blood	Healthy donor

Table 3.3: Five solid tumours samples

No	Sample type
1	E wing Sacroma
2	Hepatoblastoma
3	E wing Sacroma
4	E wing Sacroma
5	Ewing Sacroma

A total of 72 diagnostic bone marrow samples were obtained from children aged between 0 and 16 years. All of them were diagnosed with de novo acute lymphoblastic leukemia at the University of Malaya Medical Centre, Subang Jaya Medical Centre (both in Malaysia) and National University Hospital, Singapore between August 2002 -and December 2010 who were enrolled into the Malaysia-Singapore Acute Lymphoblastic Leukemia Study 2003 (MASPORE). The MASPORE protocol includes (1) Review of bone marrow slides at diagnosis, day 8, day 15 and week 5, (2) Minimal Residual Disease measurement and (3) Oncogene fusion screening. MRD was tracked in all patients treated under the MASPORE study using a simplified PCR-based marker consensus real-time quantitative PCR probes to gH, IgK and TCR rearrangements.

3.1.2 Ethical approval

Approval for this project was obtained from the University of Malaya Medical Centre Ethics committee for both the leukemia (MEC 2006/481.01) and solid tumour (MEC 2006/510.7) components.

Table 3.4: Clinical characteristics of 72 patients with ALL at diagnosis.

Characteristics	*Value (~%)*
Gender – Number (%) Male Female	 46 (64) 26 (36)
Age group – Number (%) <0 yr 1-10 yr >10 yr	 1(2) 62(86) 9(12)
Leukocyte count (x 10^9 /L) at diagnosis – Number (%) <20 20-100 > 100 *Leukocyte count at diagnosis (x 10^9 /L)* Median Range	 36 (50) 18 (75) 18(25) 20.95 0.6– 708
Blast count in bone marrow (percentage) Median Range	 90 30-90

Hemoglobin (g/L) Median Range	 8.3 2.2 – 116
Platelets (x 10^9/L) Median Range	 43 1.58 – 573

3.1.3 Tissue sample collection

Bone marrow aspiration was performed as part of diagnostic tests in these patients and as according to protocol, at day 0, 8, 15, 33 and week 12. Bone marrow samples were used for conventional diagnosis tests i.e. morphology, immunophenotyping and cytogenetic analysis. The excess materials were allocated for research works.

3.1.4 Isolation of Lymphoblasts

Materials:-

1) Ficoll-Paque Plus solution (density 1.077g/ml, Amersham Biosciences, US).
2) 1X Hanks Balanced Salt Solution-HBSS (Gibco™, 1x 0.1 micron filtered)
3) Trizol solution (Invitrogen Life Technology)
4) Conical tubes -15 ml (BD Falcon)

5) Disposable sterile transfer pipette – 3 ml
6) Neubauer haemocytometer – 0.1mm, 0.0025mm^2 ; Tiefe Depth Profondeur (Germany)
7) Light microscope (Leitz Wetzlar, Germany)
8) Table top centrifuge machine (Kubota 2420, Japan)

The bone marrow samples which were collected in ethylenediamine tetra-acetic acid (EDTA) bottles were stored at room temperature. It must be processed within two hours after the aspiration process. 4 ml of Ficoll solution was aliquot into a new 15ml conical tube. The bone marrow sample was diluted with 1x HBSS in 1:1 ratio. The tubes were inverted to make sure there were no clots. The diluted bone marrow was then layered on top of the Ficoll-solution by gently dripping the solution using sterile Pasteur pipette.

The conical tube was then centrifuged at 2000rpm/400xg for 30 minutes with rapid acceleration-slow deceleration mode. This resulted in three distinct layers. Different migration during centrifugation will form layers that contain different cell types. The lymphocytes were in the inter-phase between these two layers. The bottom layer contained erythrocytes which have been aggregated by Ficoll solution.

The cell layer was aspirated by gentle aspiration in circular motions to ensure collection of all cells at the edge of the tube and was transferred into a new 15ml Falcon tube. The tube was then top-up to 10mls HBSS for washing step. The tube was centrifuged at 1500rpm for 5 minutes. The washing step was repeated until the cell pellet appeared devoid of red cells.

Before the last wash, 10 μl of cell suspension were counted by using Neubauer chamber or haematocytometer under light microscope. After last wash, the supernatant was discarded and 1 ml of Trizol solution was added per 10 x 10^6 cells and vortexed until the cell

suspension became homogeneous. The suspension was stored at -80°C until RNA extraction.

3.1.5 RNA extraction

Materials:-

1. Isopropanol (Ajax Univar, Analytical Reagent)
2. Chloroform (Merck, Analytical Reagent)
3. 80% ethanol (Ajax Univar, Analytical Reagent)
4. Sterile nuclease free water (Amresco Inc.,OH,USA)
5. Rnase free microfuge tubes – 1.5 ml (Axygen Scientific, USA)
6. Refrigerated mini centrifuge machine (Biofuge Fresco, Heraeus).
7. Airstream vertical laminar flow (Esco Micro, Singapore)
8. Vortexer (Harmony, Japan)

9. Microcentrifuge (Cole Palmer, USA)

The sample was left at room temperature for 5 minutes to allow the cell to lyse. The sample was vortexed to homogenize the sample. The RNA extraction protocol using guanidium thiocyanate and phenol chloroform was originally developed by Chomczynski and Sacchi in 1987(Chomczynski & Sacchi, 1987). Firstly, Trizol suspension was aliquoted into 1.5ml microtube (1ml each). Subsequently, 200µl of chloroform was added into each microfuge tube. The tubes were mixed vigorously by using vortex for 15minutes, and afterwards the sample was incubated in room temperature for 2 minutes. This was followed by centrifugation at 11.2 rpm/200xg at 4°C for 15minutes.

Three distinct layers were formed after centrifugation. These consisted of a lower red phenol-chloroform phase (protein), a chalky interphase (DNA) and an upper aqueous layer containing exclusively of RNA. The aqueous layer was pipetted out carefully without touching the chalky layer, which could contaminate the RNA and transferred into a new RNase-free 1.5ml microcentrifuge tube. 500µl 100% isopropanol was added into each tube and incubated in the freezer at -20°C for 10 minutes. The tubes were centrifuged at 12000g (11200 rpm) at 4°C for 10 minutes. The step after this was performed on ice. The supernatant was discarded followed by addition of 1 ml of 80% ice cold ethanol. The suspension was mixed gently. The tube was centrifuged at 8.9 x 1000 rpm or 7500 g, 4°C for 5 minutes. The supernatant was discarded, and the remaining ethanol was removed using a pipette. The RNA pellet was air dried for 30-45 minutes. RNase-free water was added to the pellets (15-25µl). The tubes were spun briefly for 10 minutes and immediately stored in a -80^{O}C freezer.

The concentration and purity of the RNA were quantified by using ultraviolet spectrophotometer (Eppendorf Biophotometer; Hamburg, Germany). RNA concentration was automatically calculated by the spectrophotometer using the equation below:-

$$RNA\ concentration\ (\mu g/ml) = A_{260} \times 40\ \mu g/ml \times dilution\ factor$$

The measurement was done using an automated spectrophotometer and RNase free cuvettes with the reference set to sterile double distilled water in 1/50 dilution of the RNA (1 µl RNA + 49 µl sdH2O). The range of RNA purity obtained was 1.5 – 1.9. Pure RNA should have an A_{260}/A_{280} ratio of 1.9-2.1

3.1.6 Reverse Transcription PCR (RT-PCR) for Gene Expression.

Two-Step Reverse Transcription PCR

1) RT buffer -10X (Qiagen Inc., Valencia, CA)
2) dNTP mix – 5mM each dNTP (Qiagen Inc., Valencia, CA)
3) RNAse inhibitor- 50 kDa (Promega, Madison, USA)
4) Omniscript® Reverse Transcriptase (Qiagen Inc., Valencia, CA)
5) RNAse free water (Amresco Inc.,OH, USA)
6) Oligo $d(T)_{16}$ primers (New England Biolabs Inc., USA)
7) PCR flat cap tubes : 0.6ml (Axygen Scientific, USA)
8) Thermal cycler : GeneAmp® PCR System 9700 (Applied Biosystems, USA)

Complementary DNA (cDNA) was synthesized using reverse transcription technique. Initially, cDNA was synthesized by reverse transcription. The cDNA product was then used for Real-Time PCR. The reverse transcript protocol was done by using 1µg of RNA Omniscript RT Kit #205110 (Qiagen Inc., Valencia, CA). The master mix was prepared according to the following table. Then, 1µg of RNA was aliquoted into each master mix. Finally, thermal cycler was used by following the condition below.

Table 3.5: Preparation of RT-PCR master mix

Reagents	*Stock concentration*	*Final concentration*	*Volume added (µl)*
RT buffer	10x	1x	2.0µl
dNTP mix	5.0 mM	0.5 mM	2.0µl
Oligo $d(T)_{16}$ primer	10.0 µM	1.0 µM	2.0µl
Rnase inhibitor	10.0 U/µl	10.0 U/reaction	1.0µl
Omniscript RT	4.0 U/µl	4.0 U/reaction	1.0µl
RNAse free water[a]	-	-	Variable
Total RNA template[b]	Variable	1 µg / 20µl reaction	Variable
Final volume			20µl

Table 3.6: Cycling conditions for RT-PCR

Cycling condition	*Temperature*	*Time*
Reverse transcription	37 °C	60 minutes
Halt to stop reverse transcription	93 °C	5 minutes
Hold	4°C	∞

3.1.7 Conventional PCR for the assurance of cDNA quality

Materials:-

1) PCR buffer 10X – containing 15mM $MgCl_2$ (Qiagen Inc., Valencia, CA)
2) dNTP Mix – 10 mM of each nucleotide (Finnzymes, Finland)
3) DMSO (Sigma-Aldrich Co., UK)
4) HotStar Taq Polymerase – QIA#203205 (Qiagen Inc., Valencia, CA)
5) Sterile nuclease free water (Amresco Inc., OH, USA)
6) cDNA samples – refer to Table 3.8
7) Primer pairs - refer to Table 3.13 (BioBasic Inc., Canada)
8) Seakem ® LE agarose (Cambrex Bio Science)
9) Gel electrophoresis set – Sub-Cell® GT (Bio-Rad, USA)

cDNA quality was checked by using conventional PCR. The quality and concentration of the cDNA was very important to amplify the fluorescence intensity.

The same parameters from the RQ-PCR are used for the conventional PCR. The Taq DNA Polymerase #203203 was used in the PCR reaction while PCR products were viewed by using Agilent microchip. Clear distinct bands show that the cDNA were still in a good quality. Only good quality of cDNA samples were used for RQ-PCR.

Table 3.7: Preparation of conventional PCR master mix

Reagents	*Stock concentration*	*Final concentration*	*Volume added (µl)*
PCR water	-	-	17.05
PCR buffer(1.5 mM $MgCl_2$)	10X	1X	2.5
dNTPs	10mM	200µM	0.5
DMSO	100%	5%	1.25
HotStar Taq Polymerase	5U/µl	1U/reaction	0.2
Forward primer	10µM	0.5µM	1.25
Reverse primer	10µM	0.5µM	1.25
cDNA template	1000 ng	~40 ng	1

Total volume	25

Table 3.8: Cycling conditions for conventional PCR

Cycling condition	*Temperature*	*Time*	
Initial activation step	95°C	15 min	
3 steps cycling: Denaturation Annealing Extension	 94°C 60°C 72°C	 15 sec 30 sec 30 sec	35 cycles
Hold	72°C 10°C	10 min ∞	

3.1.8 Quantitative Real-Time PCR for gene expression

Materials:

1) QuantiTect SYBR Green PCR kit (Qiagen Inc., Valencia, CA)
2) Sterile nuclease free water (Amresco Inc., OH, USA)
3) Primer pairs – refer Table 3.13 (BioBasic Inc., Canada)
4) PCR flatcap 0.2 ml tubes (Molecular BioProducts Inc.,CA, USA)
5) Real-Time PCR machine: Rotor-Gene RG-3000 (Corbett Research, Australia)
6) Desktop PC, Rotor-Gene version 6.0 Application Software (Corbett Research, Australia)

TERF2 expression was measured and quantified using dsDNA intercalating dye, SYBR-Green 1(SG). The real time quantitative Polymerase Chain Reaction (RQ-PCR) was performed on a Rotorgene™ 3000 real-time thermal cycler (Corbett Research, Australia). The reagents used are stated in the table below.

Table 3.9: Reaction components for SYBR-Green Real-Time PCR

Components	*Vol/reaction*	*Final conc.*
2X Quantitect SYBR Green PCR master mix	12.5µl	1X
10µM forward primer	1.25µl	0.5µM
10µM reverse primer	1.25µl	0.5µM
Nuclease free water	9µl	-
Template cDNA (1 µg)	1µl	50 – 100 ng
Total vol.	25µl	

Step	*Temperature (°C)*	*Time*	*Notes*	*Cycle number*

PCR initial activation	95	15 min	HotStar Taq DNA Polymerase was activated by this heating step	1
Denaturation	94	15 seconds		
Annealing	60	30 seconds		60
Extension	72	30 seconds		
Melt analysis/ Data acquisition		Tm dimer < < Tm product		1

Name	*Primer*	*Sequences*
TERT	*Forward*	5’ CACGTGAGGAAGATAAACAGC 3’
	Reverse	5’ CAATGGTGGTTGGAGGATTC 3’
B2M	*Forward*	5’ GAGGCTATCCAGCGTACTCCAAAGAT 3’
	Reverse	5’ TGAAACCCAGACACATAGCAATTCAGG 3’

Table 3.10: SYBR-Green Real-Time cycling condition for Rotor-Gene

Table 3.11: The primer sequences for PCR reactions

3.2 Validation of the Method

Real-time quantitative PCR offers researchers a powerful tool for the quantitation of target nucleic acids. Methods for relative quantitation of gene expression allow us to quantify differences in the expression level of a level of a specific target (gene) between different samples. Calibrator sample and an endogenous control gene are used to normalize input amounts.

3.2.1 Selection of calibrator sample

The cell line was used as a positive control for each run to ensure there were no significant background noises. The positive control was used as a calibrator in RT-PCR calculation in *TERF2* gene expression. *TERF2* expression was quantified for few subtypes of a leukemic

cell line. Result shows HL60 cell line has a stable expression of *TERF2* gene which is used as a calibrator sample or reference gene.

TERF2 expression for the leukemic cell line was measured using a real-time assay that has been normalized with an endogenous control gene, beta-2-microglobin (*β2M*).

Table 3.12: The name of cell lines, immunophenotypes and karyotypes

Name of cell line	Immunophenotype	Karyotype
HRC57	Mature B-lymphocyte	46,XY, normal
REH	Pre-B ALL	t(12;21)(p12;q22)
SupB15	Pre-B ALL	t(9;22)(p12;q22)
697	Pre-B ALL	t(1;19)(q23;p13)
HL60	Pre-B ALL	46;XY,normal

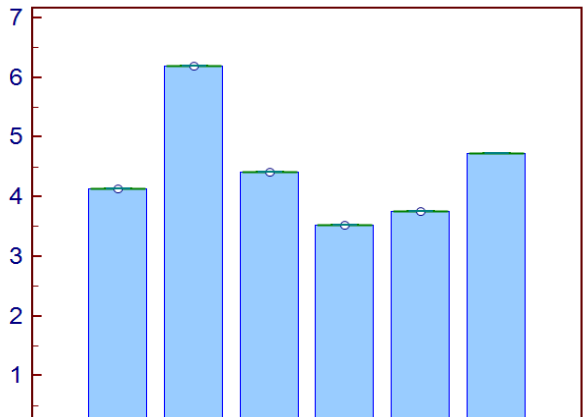

Relative expression

Cell lines

Figure 3.1: Expression of *TERF2* in different types of cell lines

3.2.2 Internal reference gene validation

In real time RT-PCR, normalization of data is one of the major steps in the analysis of gene quantification (Bustin 2002, (Pfaffl, 2001)). The reliability of RT-PCR data can be improved by normalizing it with endogenous control or also known as reference gene. Usually, cellular maintenance genes, the so-called housekeeping genes, were selected to normalize for the variability between clinical samples. The reference gene was used as a control gene because of a stable and constant expression at all stages of cell development as well as be unaffected by experimental treatments ((Bustin, 2000)).

Beta-2-microglobin (*ß2M*) is a light chain of HLA class I molecule. It is found on the surface of all nucleated cells. *β2M* is expressed in moderate level in most cells. Many researches have been conducted on the quantitative expression of *ß2M* in various genes in

different cancer cells and it was found that *ß2M* was a suitable endogenous control due to stable expression in hematopoietic cells (Lupberger et al., 2002; Vandesompele et al., 2002).

The suitability of *ß2M* as a reference gene for this study was validated by doing a RT-PCR. 10 bone marrow samples from various types of hematological malignancies. cDNA of the samples were synthesized and expression of *ß2M* was measured by using the C_T value.

Table 3.13: C_T values of *ß2M* gene for various patient diagnoses

No.	Diagnosis	C_T Value of $\beta 2M$
1	Acute myeloid leukemia	16.03
2	Acute myeloid leukemia	17.56
3	Chronic myeloid leukemia	17.53
4	Ewing sarcoma	18.14
5	Ewing sarcoma	16.08
6	Acute lymphoblastic leukemia	17.07
7	Acute lymphoblastic leukemia	17.69
8	Acute lymphoblastic leukemia	17.28
9	Congenital neutropenia	17.79
10	Viral Infection	17.42

The coefficient of variation of the *ß2M* values of the above 10 samples are

$$\frac{\text{Standard deviation}}{\text{Mean}} = \frac{0.6969 \times 100\%}{16.03} = 4.34\%$$

This was considered as an accepted amount of variability for biological samples. Hence *ß2M* was chosen as the endogenous gene for this study.

3.2.3 Relative Quantitation of gene expression

Relative quantitation of gene expression supports two experimental design and analysis methodologies; relative standard curve method and comparative C_T method ($\Delta\Delta C_T$). Comparative C_T method ($\Delta\Delta C_T$) was chosen because the standard curves for the method were not required to run on each plate. Besides, the method reduces the usage of reagents and $\Delta\Delta C_T$ is useful when a high number of samples were tested.

Thus in this study, the formula used is:

$$2^{-\Delta\Delta C_T}$$

Normalized *TERF2* expression =

$$2^{-[C_T(TERF2)-C_T(\beta 2M)]}$$

HL60 cell line was used as the calibrator cell, which stably expressed *TERF2*. The efficiencies of the target and reference gene amplification must be approximately equal for a valid $\Delta\Delta C_T$ calculation. The equation ΔC_T ($C_{T\ Target}$ - $C_{T\ reference}$) was applied for various template dilutions where finally a standard curve for both genes was generated.

The input of cDNA spanned 5 to 6 logs (i.e. 100ng to 10pg) according to the expression levels of the targets. Three replicates were required for each standard-curve point. A total of 12µl of master mix were added with 8µl of RNA.

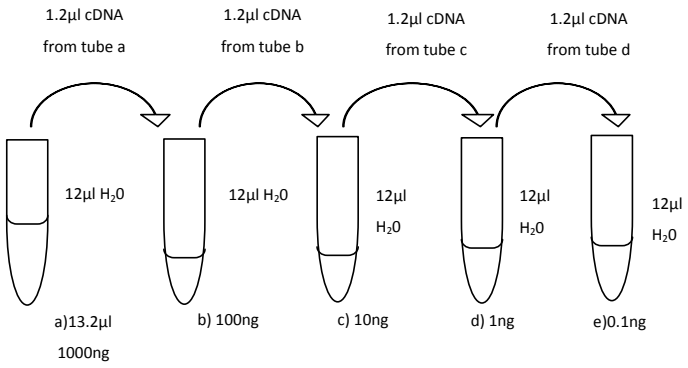

Figure 3.2: Serial dilution of the cDNA was carried out for both *TERF2* and *ß2M* gene. The serial dilution was carried out by using 10 fold dilutions. Therefore 1.2µl of cDNA from each tube was serially diluted with 12µl of RNase free water.

After the dilution, RT mix was added into each dilution tube. cDNA synthesis was carried out as described in previous page. Following, real time PCR was done by for both *TERF2* (target gene) and *ß2M* (reference gene).

In this experiment, the expression of *TERF2* was measured as a relative value to an internal reference (housekeeping gene), beta-2-microglobulin (*ß2M*. The relative quantitation of *TERF2* (target gene) and *ß2M* (reference gene) accurately determined by the comparative $\Delta\Delta\ C_T$ method according to the formula previously mentioned. PCR efficiencies of *TERF2* and *ß2M* were comparable to each other.

RNA from diagnostic bone marrow of patients was used to generate standard curves for *TERF2* and *ß2M* amplification. The PCR efficiencies value, R^2 of the two standard curves, should be approximately ~1.0.

Table 3.14: Mean values of both *TERF2* and *ß2M* genes for different log amount of cDNA

Log amount of cDNA (ng)	**Mean C_T values of *ß2M***	**Mean C_T values of *TERF2***
1000	16.47	23.73
100	19.64	26.74
10	23.34	30.19

1	27.21	34.21
0.1	30.62	38.37

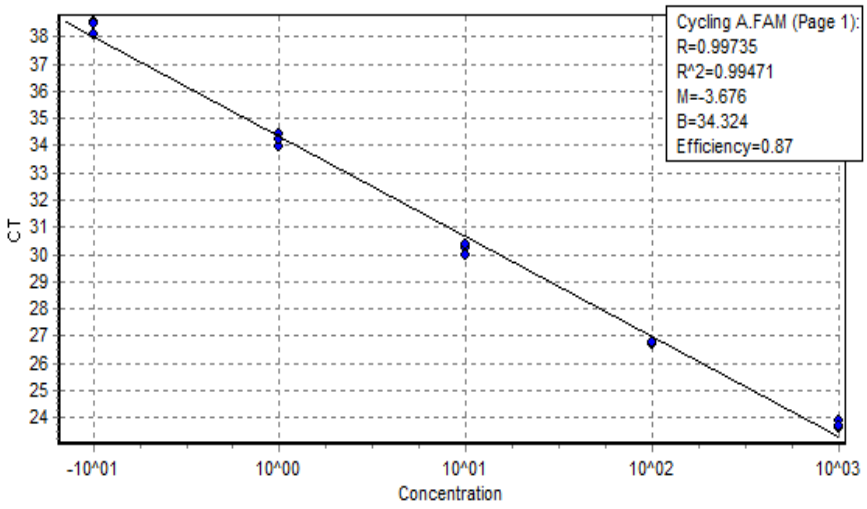

Figure 3.3: Standard curve was generated by using cDNA which was diluted over 100-fold range by real-time PCR by using *ß2M* gene specific primers.

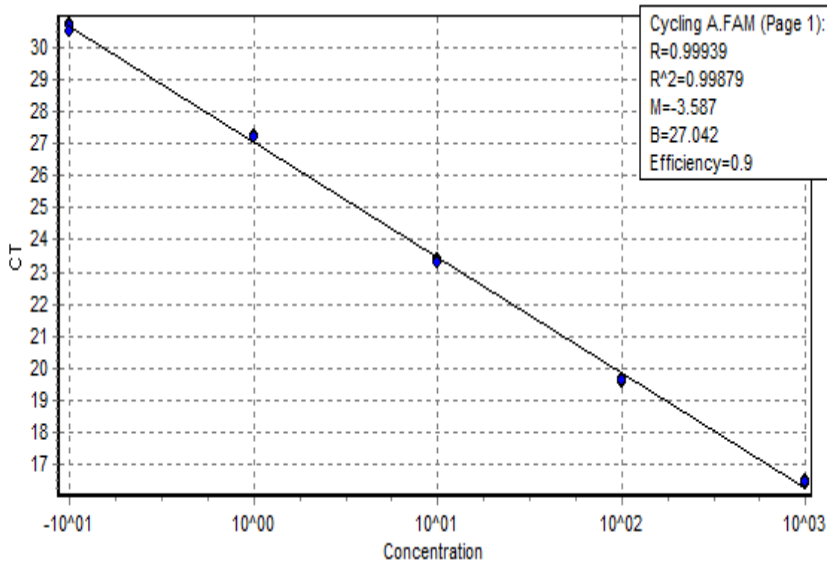

Figure 3.4: Standard curve was generated by using cDNA which was diluted over 100-fold range by real-time PCR by using *TERF2* gene specific primers.

PCR efficiency test was carried out by using 2 $^{-\Delta\Delta C}{}_{T}$ method. The efficiency of amplification of the target gene *TERF2* and internal control gene *β2M* were comparable with a correlation (R^2) value approaching 1.0. The R^2 value for both target gene *TERF2* and internal control gene *β2M* are 0.87 and 0.9 respectively.

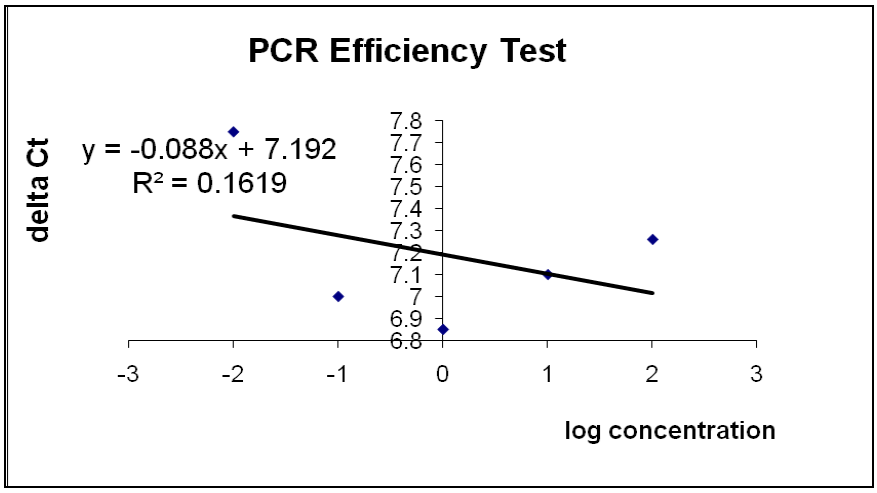

Figure 3.5: Amplification efficiency comparison of *TERF2* and *β2M*. The y-axis refers to the difference between C_T value of *TERF2* and *β2M* (delta C_T). The x-axis refers to log total cDNA (ng). The dilution series for both *TERF2* and *β2M* were prepared from cDNA sample of a patient. The delta C_T is the slope of the linear line = **- 0.088** (i.e. < 0.1) hence the amplification efficiencies were comparable between *TERF2* and *β2M*.

CHAPTER 4 – RESULTS

4.1 Main findings

TERF2 expression was quantified via real-time PCR assay by using Rotorgene™ 3000 thermalcycler (Corbett Research, Australia) and SYBR-Green™ (Qiagen,Valencia CA,USA) as the fluorescent probe. Telomeric repeat binding factor 2 (*TERF2*) expression was compared with various samples; control samples (free from hematological diseases), other type of hematological malignancies (AML, and CML), solid tumour samples and acute lymphoblastic leukemia samples. *TERF2* was found to be highly expressed in acute lymphoblastic leukemia samples. *TERF2* gene expression successfully discriminated ALL from other hematological malignancies (AML and CML) as well as solid tumours .

Firstly, the D'Agostino-Pearson test was carried out by using MedCalc® version 11.3.8.0 to check for normal distribution of the data. The normality is rejected with P=0.088. The distribution was generated using histogram with different expression points.

There was a wide spectrum of relative *TERF2* expression, ranging from 0.0072 to 4.2575 (mean=0.5736, median=0.5664). The distribution of relative *TERF2* expression is shown below. The distribution curve does not show a normal distribution.

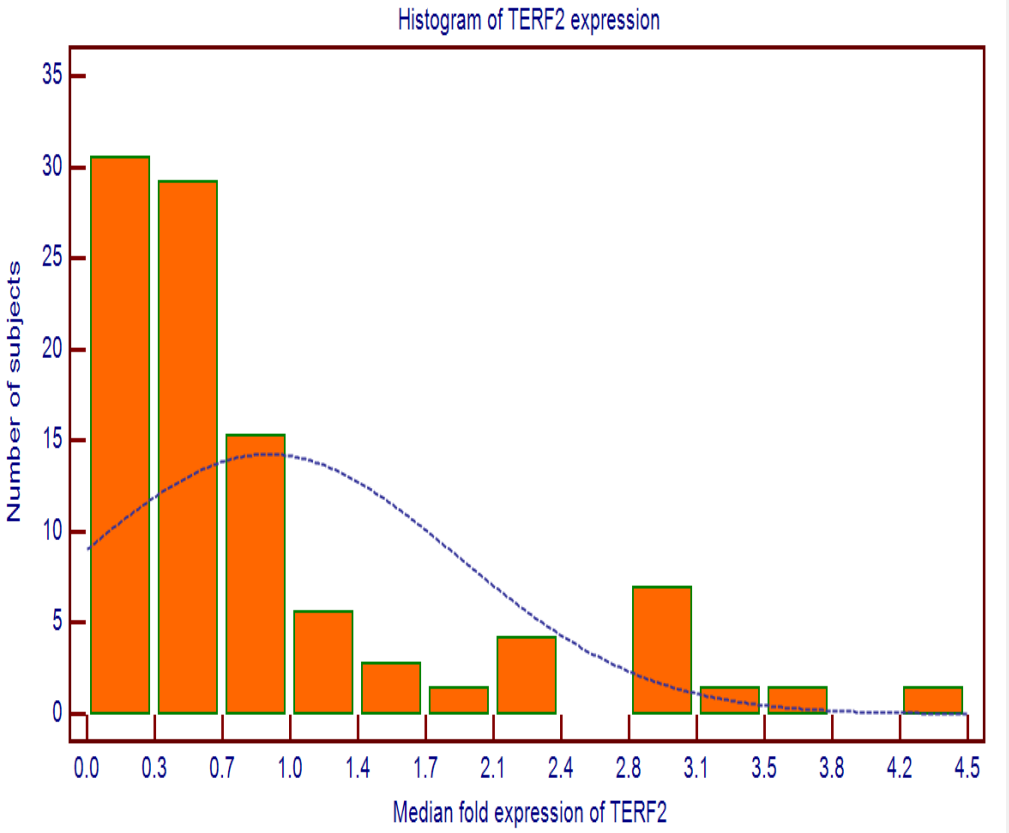

Figure 4.1: Histogram showing *TERF2* expression in diagnostic marrow samples in 72 patients with acute lymphoblastic leukemia. The x-axis refers to the median fold expression of *TERF2*. All samples were run in triplicates and measured using real-time quantitative PCR. The y-axis shows the number of patients with a particular value of *TERF2* expression.

Expression of *TERF2* in diagnostic bone marrow samples of children with ALL were compared with control samples (refer Table 3.2). Mann-Whitney U test was used to show that there was no difference between the *TERF2* gene expressions of the two groups. The p value was p=0.0350, thus, the null hypothesis was rejected as there was a significant difference in *TERF2* expression between normal samples and ALL diagnosis samples. The box and whisker plots showed that *TERF2* expression in ALL, is significantly higher than control samples ($p<0.05$).

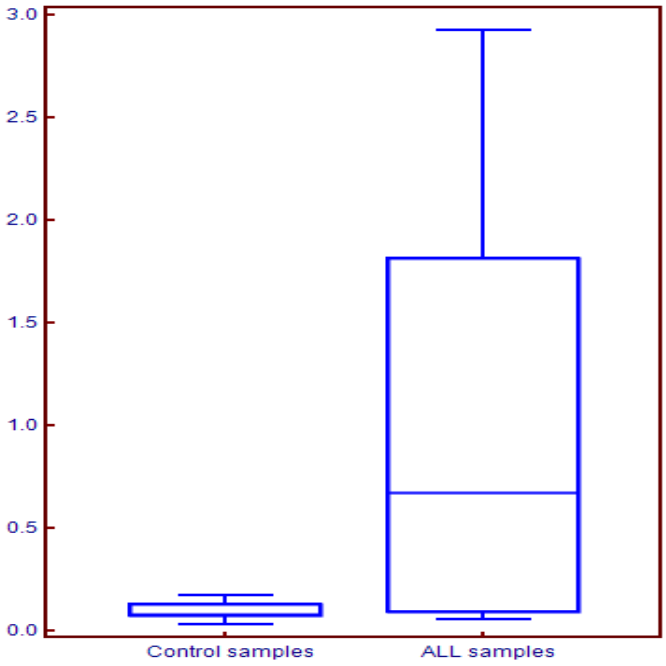

Figure 4.2: *TERF2* gene expression of the diagnostic bone marrow in childhood acute lymphoblastic leukemia (Control samples=10; ALL samples=10). Mann-Whitney U tested out by using MedCalc® version 11.3.8.0.

TERF2 expression in ALL in comparison to healthy bone marrow, various types of hematological malignancies (AML, CML, JMML) and solid tumour samples were quantified. The median *TERF2* expression was significantly higher in ALL diagnostic bone marrow samples compared to the others. *TERF2* gene expression successfully discriminated ALL from other hematological malignancies (AML and CML) and solid tumours samples (refer Table 3.3).

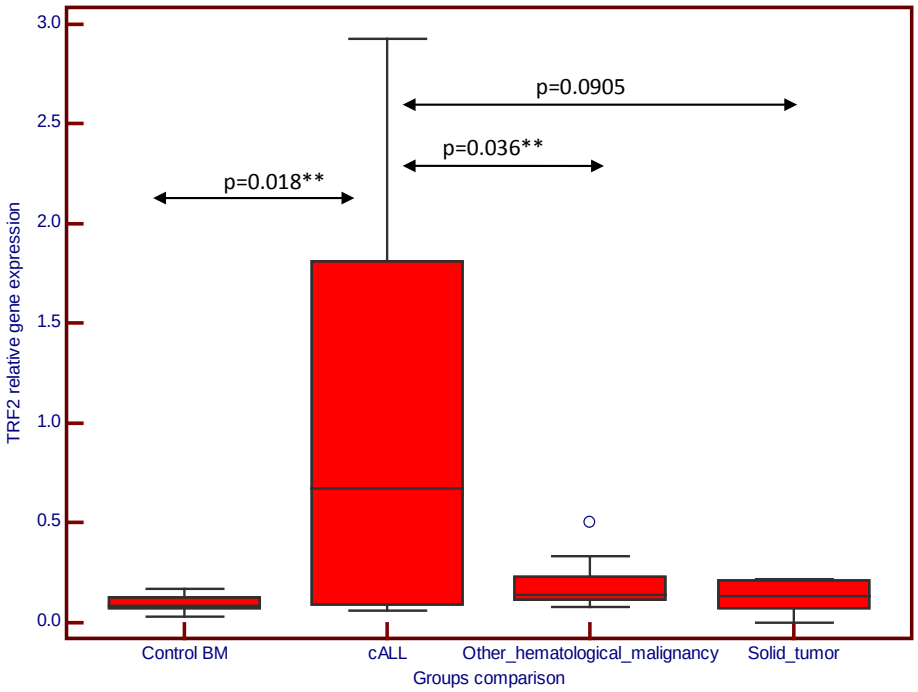

Figure 4.3: The box and whisker plot presents the relative fold of *TERF2* expression in 33 samples from different groups. The x-axis refers to the various groups while the y-axis refers to fold expression of *TERF2* relative to HL60 (calibrator). The box whisker plot is generated based on median values of the gene expression.

TERF2 expression was measured within subgroups of 72 ALL samples. A box and whisker plot was generated by using MedCalc® version 11.3.8.0 to represent the data.

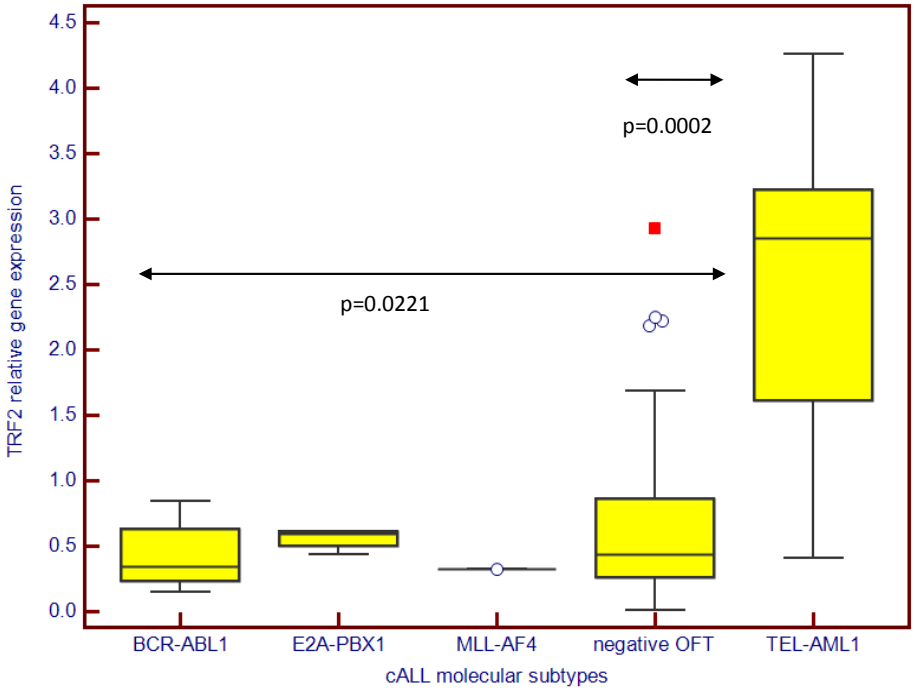

Figure 4.4: The box and whisker plot demonstrates the relative fold *TERF2* expression in 72 diagnosis marrows in ALL with different cytogenetic subtypes; 'negative OFT' = no fusion transcript detected; BCR-ABL1=t(9;22); E2A-PBX1=t(1;19); MLL-AF4=t(4;11) and TEL-AML1=t(12;21). The x-axis refers to the various ALL cytogenetic subtypes while the y-axis refers to relative expression of *TERF2* by using HL60 as calibrator gene.

The result shows that the TEL-AML1 subgroup had higher median expression levels of *TERF2*. The median expression levels of *TERF2* in different group of subgroups were: BCR-ABL, 0.3439; TEL-AML1, 2.8481; E2A-PBX1, 0.591; MLL gene rearrangements, 0.3209 and those without any fusion transcripts, 0.8706.

4.2 Determining Cut-Off Value of TERF2 Expression

The cut-off value for *TERF2* expression was validated using the receiver operating curve (ROC) analysis. Only fifty-four samples were only included due to data insufficiency for the day 33 remission status. First of all, all cases were labeled as achieving remission at day 33 of therapy or. Patients who achieved remission were labeled as event (n=0) and those who does not achieve remission were labeled as a non-event (n=1).

The ROC curve was generated by using MedCalc® version 11.3.8.0. The cut off point value was used to discriminate over-expression or under-expression of *TERF2*. The cut off value generated was 0.3439. Patients who have an expression less than 0.3439 were declared as *TERF2* under-expression and over-expression for those who have higher expression than 0.3439.

It was found that patients who did not over-express *TERF2* were also not likely to achieve remission at end of induction therapy. Of seventeen patients who did not overexpress *TERF2* under-expressed *TERF2,* 14 (82.35%) did not achieve clinical remission at day 33. In contrast, of 37 who over-expressed *TERF2,* 11 of them achieved clinical remission at day 33 (29.73%).

Following this, the area under the curve was determined with 0.663 having significance level of P 0.0273 (P< 0.005) (95% CI 0.521, 0.786).

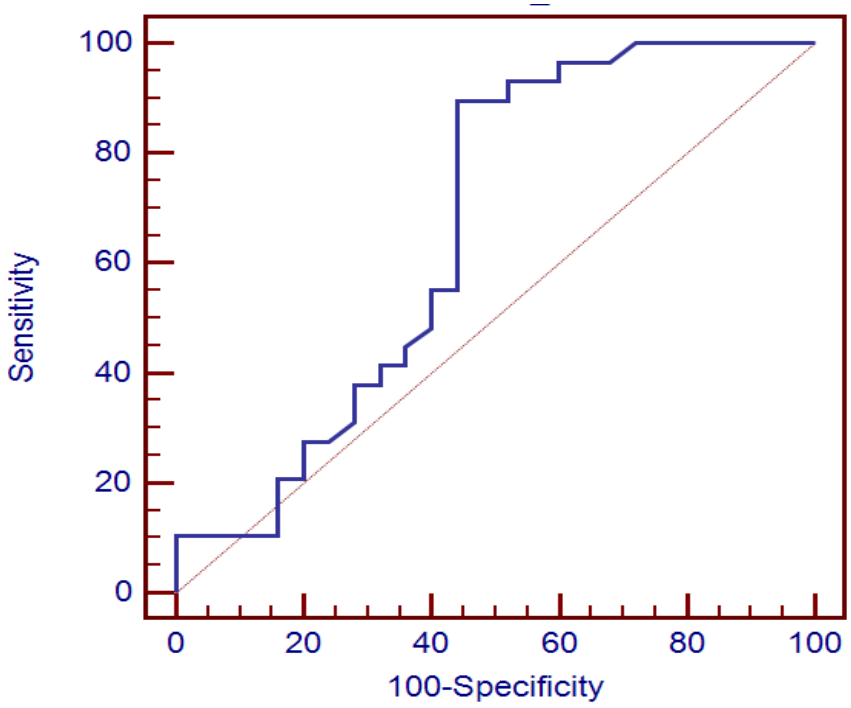

Figure 4.5: Receiver operating curve analysis was conducted to determine the cut off point for the median fold expression of *TERF2* in diagnosis bone marrow samples. The x=axis refers to the percentage likelihood of not obtaining a false positive result. The y-axis refers to the percentage likelihood of obtaining a true positive result. Graph was generated by using MedCalc® version 11.3.8.0 software.

According to the graph below, the data of the negative and positive groups was displayed as dots on two vertical axes. A horizontal line indicates the cut-off point with the best separation (minimal false negative and false positive results) between the two groups. The corresponding test characteristics *sensitivity* and *specificity* were shown at the right side of the graph.

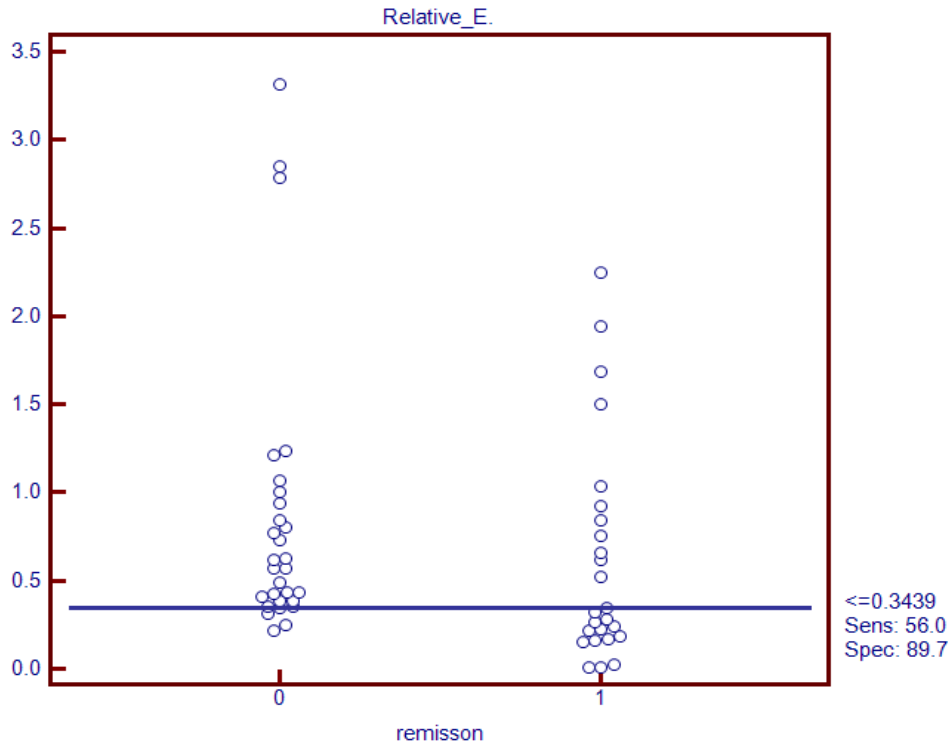

Figure 4.6: Dot diagram shows 0.3439 is the cut off point to determine whether the patients overexpress *TERF2* . Two distinct group show whether the patients have achieved clinical remission at day 33 (0) or not (1). The result clearly shows that patients who do not achieve remission at day 33 were underexpressed *TERF2* expression if compared to patients who achieved clinical remission at day 33.

4.3 Survival Curves

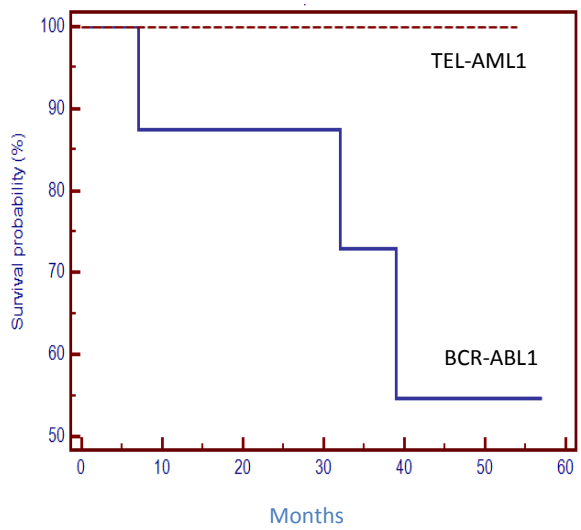

Figure 4.7 : Kaplan Meier survival curve for 18 patients treated in UMMC under the MASPORE ALL 2003 trial; 8 (BCR-ABL1) and 10 (TEL-AML1). Figure shows TEL-AML1 patiens have a better prognosis than the BCR-ABL1 patients.

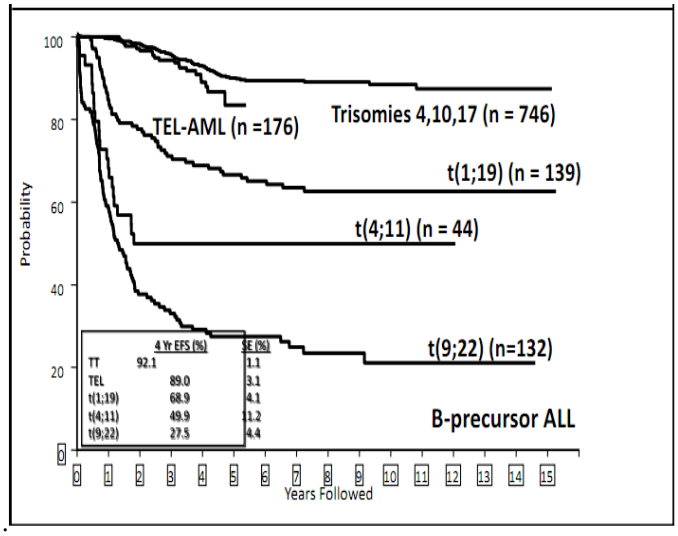

Figure 4.8: Genotype correlates with the outcome of the patients (Legacy Children's Oncology Group). Data shows TEL-AML1 patients have a better prognosis than BCR-ABL1 patients. (Mignon, 2011)

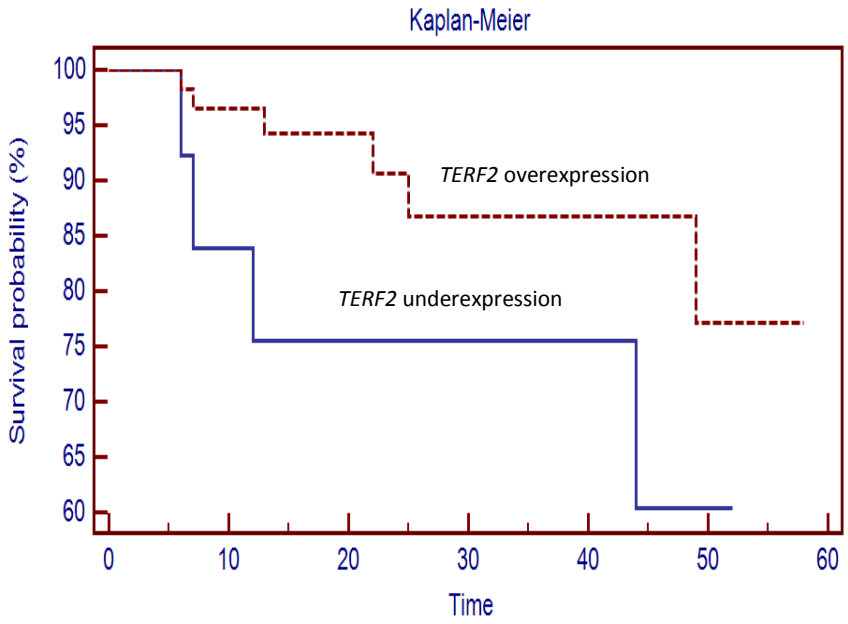

Figure 4.9: Kaplan-meier analysis of relapse-free survival in 72 ALL patients were stratified according to the higher and lower expression of *TERF2* in their diagnosis bone marrow samples taken at diagnosis. The x-axis refers to the period of follow-up (months) and the y-axis refers to the proportion of patients. The dashed and dark lines refer to patients who over-expressed *TERF2*, or not respectively .

4.4 Expression of TERF2 and clinical parameters

Analysis of co variance (ANCOVA) was carried out to determine the relationship between the over-expression of *TERF2* with other clinical parameters. Analysis of covariance allows us to compare one variable in 2 or more groups by taking into account the covariates.

Levene's test for equality of variance is performed before ANCOVA test. If the calculated P-values for the two main factors A and B or for the 2-factor interaction are less than the conventional 0.05 (5%), then the corresponding null hypothesis is rejected, and the alternative hypothesis is accepted indicating that there are differences among groups.

The clinical parameters for poor risk features i.e. high presenting leucocyte count ($50x10^9$/L), infants, and oncogene fusion, *BCR-ABL1* and *MLL-AF4*, were used in this study. On the other hand, the occurrence of relapse was used to determine the survival advantage in patients. These clinical parameters were analysed with the *TERF2* over- and under-expressions.

Table 4.1: Analysis of co variance (ANCOVA) was conducted to determine the relationship between the expression of *TERF2* with clinical parameters.

Clinical parameters	***TERF2* over expression (37)**	***TERF2* under expression (17)**	***P* value**
Age <2 years	29 (29.41%)	12 (70.59%)	0.7
Leucocytosis $> 50x10^9$/L	15 (40.54%)	6 (35.29%)	0.9
Poor risk	3 (8.1%)	5 (29.41%)	0.09

CHAPTER 5: DISCUSSION AND CONCLUSION

Progress in the treatment of childhood acute lymphoblastic leukemia (ALL) has been excellent. However, despite the impressive improvement in patients outcome, relapsed ALL remains the foremost pediatric malignancy, occurring more frequently than newly-diagnosed acute myeloid leukemia or most solid tumours (Harned & Gaynon, 2008). Currently, pediatric patients with ALL have a complete remission rate (CR) of 95% with an estimated 5-year event-free survival (EFS) rate of 80-85% (Advani, 2010).

Despite this success, an estimated 350 to 500 individuals die each year from ALL, with most suffering one or more relapses before death. The number of deaths from ALL is equivalent to or more than the total incidence of many other childhood cancers, including neuroblastoma, retinoblastoma, Wilm's tumour, osteosacroma, Ewing's sarcoma, rhabdomyosacroma, thyroid carcinoma, and melanoma (Reaman et al., 1993; Wells, 2008). This outcome is unsatisfactory and indicates that the treatment available to children who relapsed is, in general, unsatisfactory. In addition, obtaining reliable data on the incident and outcome following leukemia relapse is difficult because relapse may occur soon after initial treatment begins, or up to many years (2- to 3-years) after treatment is completed or any time in between these points (Wells, 2008).

The Cancer Research UK Children's Cancer Group prospectively analyzed and correlated the gene expression profiles of children presenting with acute leukemia from the Royal London and Great Ormond Street Hospitals with morphological diagnosis, immunophenotype and karyotype. Total RNA was extracted from blast cells which was obtained from 84 acute lymphoblastic leukemia patients and hybridized to the high density

Affymentrix U133A oligonucleotide array. A common profile for children with ALL with a *TEL-AML1* fusion was identified (Bellotti et al., 2005). The *TERF2* gene was most highly expressed in this group of patients (Bellotti, et al., 2005). Thus, we chose *TERF2* to investigate the possible role of the gene in ALL as well as explored its potential as a therapeutic or prognostic target.

TERF2 is a key regulator of telomere protection and telomere length (van Steensel, Smogorzewska, & de Lange, 1998); two processes that are essential for chromosomal stability. In addition, *TERF2* interacts with several DNA repair factors, as well as DNA damage signaling protein, most of which are involved in human chromosome instability syndromes characterized by premature aging and increased cancer risk (Blasco, 2005). The fact that *TERF2* is over-expressed in a variety of cancers (skin, lung, liver, and breast) (Artandi & DePinho, 2010; Blanco, et al., 2007; Harley et al., 1994) suggests a role for *TERF2* in carcinogenesis. The results are similar with recent findings suggesting that *TERF2* loss of function reduces the tumourigenicity of human malignant cell lines (Blanco, et al., 2007).

After successfully developing and validating a real-time quantitative assay for *TERF2*, we studied diagnostic bone marrow samples from 72 ALL patients recruited into our trial. Over-expression of *TERF2* was noted in those with TEL-AML1 fusion, a subgroup historically associated with good outcome.

Our finding of *TERF2* over-expression in the *TEL-AML1* subgroup is concordant with the microarray data from other research groups (van Delft et al., 2005; Yeoh et al., 2002). *TERF2* is one of the 40 genes that are useful to discriminate ALL from AML (van Delft, et al., 2005). We found that *TERF2* upregulation occurs significantly only in patients positive

for *TEL-AML1*. In contrast, down regulation of *TERF2* occurs in high risk group of cALL namely; *BCR-ABL1* and *MLL-AF4*. However, our findings are opposite to that of the UK Cancer Research group (van Delft, et al., 2005) in which they reported that *TERF2* was significantly upregulated in *BCR-ABL1* positive patients. We hypothesize that over-expression of *TERF2* in *TEL-AML1* would serve as a protective mechanism for the telomere from end to end fusion by preventing anaphase bridges from occurring and subsequently, this will promote chromosomal stability (Cookson & Laughton, 2009).

When exposed to chemotherapeutic agents and with the presence of intact telomere maintenance function, *TERF2* triggers normal apoptosis and DNA damage mechanism via ataxia-telangiectasia mutated (ATM) and p53 signaling pathway checkpoints (Maser & DePinho, 2002). This may explain why most of the *TEL-AML1* patients respond well to standard chemotherapy and usually will achieve complete remission by day 33.

Hypomethylation of promoter and exon 1 CpG islands of *TERF2* gene may be one of the important epigenetic mechanisms in which *TERF2* gene can be over-expressed. However, this is not the only mechanism involved in *TERF2* regulation (Dong, Wang, Chen, Sun, & Wu, 2010). In *TEL-AML1* cells, it has been reported from genome wide analysis studies that *TERF2* as well as other genes (MCM3, MCM4, MCM5, CDC23) involved in proliferation decreased significantly after it has been exposed to L-asparaginase (Fine, Kaspers, Ho, Loonen, & Boxer, 2005). This might explain why TEL-AML1 cell responses well towards the L-asparginase.

In contrast to TEL-AML1 blasts, blasts with the BCR-ABL1 translocation show different characteristics. We speculate that *TERF2* is under expressed in *BCR-ABL1* cells because *TERF2* only acts when there is a need to protect shortened telomeres. *TERF1*,

TERF2 and TIN2 are negative regulators of the telomere length (Houghtaling, Cuttonaro, Chang, & Smith, 2004). It has been reported that in complex or advanced cancer stage, telomere length is abnormal and longer than usual as a result of alternative lengthening telomere (ALT), creating dysfunctional telomere (Reddel, 2003; Wellinger, Ethier, Labrecque, & Zakian, 1996). We hypothesize that BCR-ABL1 cells carry a longer telomere which eventually switches off the expression of *TERF2*. *TERF2* under expression will not be able to protect the telomere causing more serious complications to the chromosomes, thus impairing genomic stability.

Malignant cancer cells usually have very long telomeres at the late stage of neoplasia (Artandi & DePinho, 2010). Initially, telomerase and its' subunits were known to lengthen the telomere structure causing immortalization in malignant cancer cells. There have been some controversial issues with current telomerase inhibitors which have been found to not be effective in treating certain cancers. This is because telomerase and its subunits are independent of the telomere length (Bryan, Marusic, Bacchetti, Namba, & Reddel, 1997). Telomere length can be altered by the ALT mechanism, which regenerate telomeres in the absence of telomerase and potentially endow cancer cells with an escape from crisis (Bryan, Englezou, Dalla-Pozza, Dunham, & Reddel, 1997). Thus, the promising way to solve this problem is by targeting telomere maintenance genes including RAP1 *TERF2*1, *TERF2* and POT1 which all play roles in the ALT pathway.

Many authors have studied the role of telomere, telomerase and telomere maintenance genes in chronic leukemias and acute myeloid leukemias but few reported the role of *TERF2* regulation in cALL and none focused in the specific molecular subtypes of cALL. Due to funding limitations, we only manage to investigate the potential role of *TERF2* in cALL biology. Hence, further investigation needs to be done to confirm the exact

mechanism in elucidating the correlation of telomere, telomerase and telomere maintenance genes in different cALL subtypes.

In conclusion, telomere haemostasis has been significantly deregulated in cALL, and each molecular subtype has different *TERF2* gene deregulation. Our results suggest that *TERF2* has a potential prognostic implication, which may serve as a potential therapeutic strategy tool in the different molecular subtypes in cALL.